## Study of $\Lambda(1405)$ in photoproduction of $K^*$

T. Hyodo, A. Hosaka, M. J. Vicente Vacas, and E. Oset

<sup>1</sup>Research Center for Nuclear Physics (RCNP), Ibaraki, Osaka 567-0047, Japan <sup>2</sup>Departmento de Física Teórica and IFIC, Centro Mixto Universidad de Valencia-CSIC, Institutos de Investigación de Paterna, Aptd. 22085, 46071 Valencia, Spain (Dated: December 16, 2018)

We investigate the photoproduction of  $K^*$  vector meson for the study of the  $\Lambda(1405)$  resonance. The invariant mass distribution of  $\pi\Sigma$  shows a different shape from the nominal one, peaking at 1420 MeV. This is considered as a consequence of the double pole structure of  $\Lambda(1405)$ , predicted in the chiral unitary model. Combined with other reactions, such as  $\pi^- p \to K^0 \pi\Sigma$ , experimental confirmation of this fact will reveal a novel structure of the  $\Lambda(1405)$  state.

PACS numbers: 13.60.-r, 13.88.+e, 14.20.Jn Keywords: chiral unitary approach,  $\Lambda(1405)$ 

The structure of the  $\Lambda(1405)$  resonance has been a long-standing problem in hadron physics. As is well known, it is not easy to derive a proper mass for  $\Lambda(1405)$ in a naive quark model, while unitary coupled channel approaches [1, 2, 3], in which the resonance is described as a quasi-bound state of a meson and a baryon, have been successful. In recent years, these issues are reconsidered on the basis of chiral effective Lagrangians and fundamental QCD. The chiral unitary model [4, 5, 6, 7], which implements the interaction derived from chiral perturbation theory and coupled channel unitarity, has been well reproducing the S = -1 meson-baryon scattering amplitude, generating  $\Lambda(1405)$  dynamically. One of the lattice QCD calculations has reported the difficulty in describing  $\Lambda(1405)$  by three-quark interpolating operator [8]. These facts seem to favor the meson-baryon picture of the  $\Lambda(1405)$  state, rather than a simple 3-quark state.

In this study, we focus on the pole structure of the  $\Lambda(1405)$  resonance; it has been found that there are two poles in the region of  $\Lambda(1405)$  through analyses based on the chiral unitary models [9, 10, 11, 12, 13, 14, 15, 16]. The conclusion does not depend on the details of the models, qualitatively. The existence of two poles was first found in the cloudy bag model [17]. Very recently, a study of  $1/2^-$  pentaquark states with correlated diquark picture [18] also reported two  $\Lambda$  states at relatively low energy region.

The detailed structure of these poles have been studied in the chiral unitary model, which we use in this study. For instance, in Ref. [19], the positions of the poles and its coupling strengths to meson-baryon channels are calculated as in Table. I. We see that the pole  $z_1$  couples dominantly to  $\pi\Sigma$  channels, while  $z_2$  couples dominantly to  $\bar{K}N$  channels. Under this situation, the shape of  $\Lambda(1405)$  seen in invariant mass distribution of  $\pi\Sigma$  should depend on the reaction to generate the resonance. In fact, such differences were seen in previous theoretical studies [20, 21, 22]. It was found in Ref. [22] that the  $z_1$  pole was favored in the  $\pi^-p \to K^0\pi\Sigma$  reaction.

In this paper, we propose  $\gamma p \rightarrow K^*\Lambda(1405) \rightarrow$ 

TABLE I: Pole positions and coupling strengths  $g_i$  for several channels in the chiral unitary model [19].

pole	$\pi\Sigma$	$\bar{K}N$	$\eta\Lambda$	KΞ
$z_1 = 1390 - 66i$	2.9	2.1	0.77	0.61
$z_2 = 1426 - 16i$	1.5	2.7	1.4	0.35

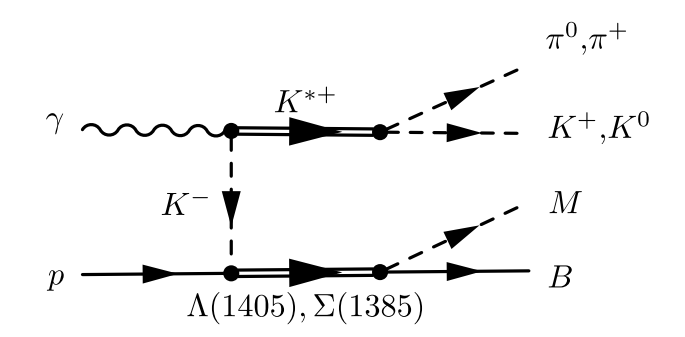


FIG. 1: Feynman diagram for the reaction. M and B denote the meson and baryon of ten coupled channels of S=-1 meson-baryon scattering. In this paper we only take  $\pi\Sigma$  and  $\pi\Lambda$  channels into account.

 $\pi^+ K^0 MB$  reaction in order to isolate the  $z_2$  pole. The advantages of this reaction are

- In K exchange diagram as shown in Fig. 1, the pole  $z_2$  will be selected, because  $\bar{K}N$  channel couples to  $\Lambda(1405)$  at initial stage.
- We can select the above events, using the correlation between polarization of photon beam and angular distribution of final  $\pi^+K^0$  [23].

In the present calculation, we consider the threshold production of  $K^*$  and  $\Lambda(1405)$ , and utilize the s-wave meson-baryon scattering amplitude calculated by the chiral unitary model [10, 13], as the final state interaction of  $\bar{K}N$ . In order to perform a realistic calculation, we introduce the p-wave  $\Sigma(1385)$  field explicitly.

The scattering amplitude as described by the diagram



FIG. 2: Feynman diagram for  $K^-p \to MB$ .

of Fig. 1 can be divided into two parts

$$-it = (-it_{\gamma \to K^- K\pi}) \frac{i}{p_{K^-}^2 - m_{K^-}^2} (-it_{K^- p \to MB}) . \quad (1)$$

The former part  $(-it_{\gamma \to K^-K\pi})$ , is derived from the effective Lagrangians [23], and given as

$$-it_{\gamma \to K^- K^0 \pi^+} = \frac{i\sqrt{2}g_{VPP}\epsilon^{\mu\nu\alpha\beta}p_{\mu}(K^0)p_{\nu}(\pi^+)k_{\alpha}(\gamma)\epsilon_{\beta}}{P_{K^*}^2 - M_{K^*}^2 + iM_{K^*}\Gamma_{K^*}},$$
(2)

where p and k are the momenta of the particle in parentheses,  $\epsilon_{\mu}$  the polarization vector of photon,  $g_{VPP}=-6.05$  the universal vector meson coupling, and  $\Gamma_{K^*}$  the total decay width of  $K^*$ , for which we take the energy dependence into account. It is easy to see the  $\pi^+K^0$  distribution is correlated with the polarization of initial photon.

The amplitude  $(-it_{K^-p\to MB})$ , shown in Fig. 2, consists of two parts

$$-it_{K^-p\to MB}(M_I) = -it_{ChU}(M_I) - it_{\Sigma^*}(M_I) , \quad (3)$$

where  $-it_{ChU}$  is the meson-baryon scattering amplitude derived from the chiral unitary model, and  $-it_{\Sigma^*}$  is the  $\Sigma(1385)$  pole term.  $M_I$  is the invariant mass for  $K^-p$  system, which is determined by  $M_I^2 = (p_{\gamma} + p_N - p_{K^*})^2$ . In the chiral unitary model [10, 13], the coupled channel amplitudes are obtained by

$$t_{ChU}(M_I) = [1 - VG]^{-1}V,$$
 (4)

where G is the meson-baryon loop function and V is the kernel interaction derived from the Weinberg-Tomozawa term of the chiral Lagrangian. The  $\Sigma(1385)$  term is introduced with couplings  $c_i$  to channel i ( $\Sigma(1385) \to MB$ ) which are deduced from the  $\pi N\Delta$  using SU(6) symmetry, and explicit values are shown in Ref [23]. Then we have the amplitude

$$-it_{\Sigma^*}(M_I) = -c_1 c_i \left(\frac{12}{5} \frac{g_A}{2f}\right)^2 \mathbf{S} \cdot \mathbf{k}_1 \mathbf{S}^{\dagger} \cdot \mathbf{k}_i$$

$$\times \frac{i}{M_I - M_{\Sigma^*} + i\Gamma_{\Sigma^*}/2} F_f(k_1) ,$$
(5)

where  $g_A = 1.26$ ,  $f = 93 \times 1.123$  MeV [10] and S is a spin transition operator. We have introduced a strong form factor  $F_f(k_1) = (\Lambda^2 - m_K^2)/(\Lambda^2 - k_1^2)$  with  $\Lambda = 1$  GeV, for the vertex  $K^-p\Sigma^*$  in order to account for the finite size structure of the baryons.

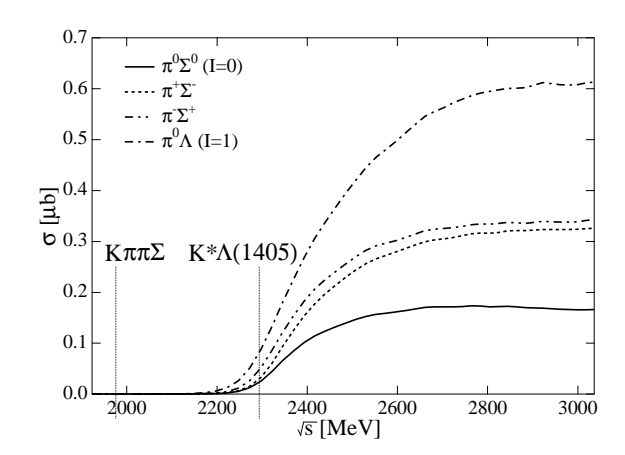


FIG. 3: Total cross sections of the process with the final states  $\pi^0\Sigma^0$  (Solid),  $\pi^+\Sigma^-$  (Dashed),  $\pi^-\Sigma^+$  (Dash-dot-dotted) and  $\pi^0\Lambda$  (Dash-dotted) in units of  $[\mu b]$ . Solid bars indicate the threshold energy of channels.

The cross section is given as a function of the incident energy  $\sqrt{s}$ :

$$\sigma(\sqrt{s}) = \frac{2MM_{\Sigma}}{s - M^2} \int \frac{d^3p_1}{(2\pi)^3} \frac{1}{2\omega_1} \int \frac{d^3p_2}{(2\pi)^3} \frac{1}{2\omega_2} \times \frac{1}{2} \int_{-1}^{1} d\cos\theta \frac{1}{4\pi} \frac{\tilde{P}_3}{M_I} |t(\cos\theta)|^2 ,$$
 (6)

where  $p_{1(2)}$  and  $\omega_{1(2)}$  are the momenta and energy of the final  $K(\pi)$  from  $K^*$ , and  $\tilde{P}_3$  is the relative three momentum of MB ( $\sim \pi \Sigma$  or  $\pi \Lambda$ ) in their center of mass frame. The angle  $\theta$  denotes the relative angle of MB in the CM frame of the total system. The calculation is performed by the Monte-Carlo method.

Before going to the numerical results, here we mention the MB channels decaying from the intermediate baryonic states  $(B^* \sim \Lambda(1405), \Sigma(1385))$ , below the threshold of the  $\bar{K}N$  channel. In the present case, since we have the  $K^-p$  channel initially, the I=2 component of  $\pi\Sigma$  channel is not allowed, and hence, there are two charged and two neutral channels. Considering the Clebsh-Gordan coefficients [20], the charged channels  $(\pi^{\pm}\Sigma^{\mp})$  are from the decay of both  $\Lambda(1405)(I=0)$  and  $\Sigma(1385)(I=1)$ , while the neutral channels are from either one of the two;  $\pi^0\Sigma^0$  is from  $\Lambda(1405)$  and  $\pi^0\Lambda$  is from  $\Sigma(1385)$ .

In Fig. 3, we show the total cross sections  $\sigma(\gamma p \to K^*B^* \to \pi^+ K^0 MB)$  as functions of  $\sqrt{s}$  for different MB channels. The use of polarized beam enables us to reduce possible backgrounds, but there is not distinction between cross sections of polarized and unpolarized processes, unless we observe angular distributions. In the figure,  $\pi\Lambda(I=1)$  channel gives the largest magnitude, which might disturb the I=0 amplitude, that we are interested in. However, as we see below, it is possible to isolate  $\Lambda(1405)$  from  $\Sigma(1385)$  contribution, with proper combination of final states.

In Fig. 4, we show the invariant mass distributions for different decay channels with photon energy  $E_{\gamma} = 2500$ 

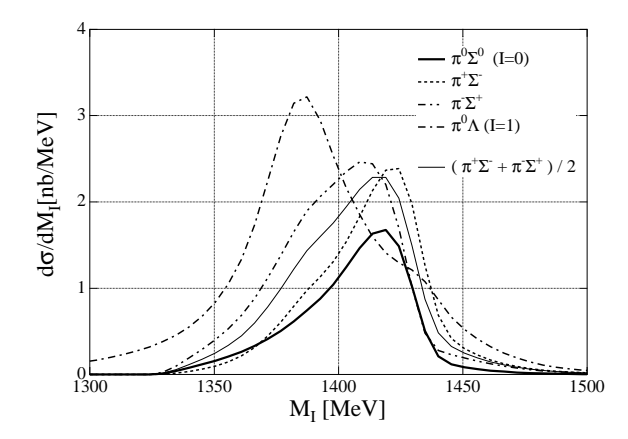


FIG. 4: Invariant mass distributions of  $\pi^0\Sigma^0$  (Thick solid),  $\pi^+\Sigma^-$  (Dashed),  $\pi^-\Sigma^+$  (Dash-dot-dotted),  $\pi^0\Lambda$  (Dash-dotted) and  $(\pi^+\Sigma^- + \pi^+\Sigma^-)/2$  (Thin solid) in units of [nb/MeV]. Initial photon energy in Lab. frame is 2500 MeV ( $\sqrt{s} \sim 2350$  MeV, threshold of  $K^*\Lambda(1405)$ ).

MeV (the threshold for  $K^*\Lambda(1405)$  production is 2350 MeV). As expected, the  $\pi^0 \Sigma^0$  distribution decaying from  $\Lambda(1405)$  (Thick solid line) has a peak around 1420 MeV which is the position of the  $z_2$  pole. The  $\pi^0\Lambda$  distribution (dot-dashed line) has clearly a peak around 1385 MeV. Forgetting about the experimental feasibility, these neutral channels are most helpful in order to distinguish the contributions from  $\Lambda(1405)$  and  $\Sigma(1385)$ , since they are pure I = 0 or 1. In experiments, the charged states (dashed and dash-dot-dotted lines) may be observed, which contain both  $\Lambda(1405)$  and  $\Sigma(1385)$  contributions. The shapes of the three  $\pi\Sigma$  distributions have a similar tendency as the Kaon photoproduction process [20], which has been confirmed in experiments [24]. Note also that the contributions from  $\Sigma(1385)$  seem to be small for these channels.

It is worth showing the isospin decomposition of the distributions of charged states [20]

$$\frac{d\sigma(\pi^{\pm}\Sigma^{\mp})}{dM_{I}} \propto \frac{1}{3}|T^{(0)}|^{2} + \frac{1}{2}|T^{(1)}|^{2} \pm \frac{2}{\sqrt{6}}\operatorname{Re}(T^{(0)}T^{(1)*});$$

$$\frac{d\sigma(\pi^{0}\Sigma^{0})}{dM_{I}} \propto \frac{1}{3}|T^{(0)}|^{2},$$
(7)

where  $T^{(I)}$  is the amplitude with isospin I. This equation tells us that the difference between  $\pi^+\Sigma^-$  and  $\pi^-\Sigma^+$  comes from the crossed term  $\mathrm{Re}(T^{(0)}T^{(1)*})$ , and when we sum up the two distributions, this term vanishes. In Fig, 4, we show the result of average of the charged  $\pi\Sigma$  channels (thin solid line), in order to remove the contribution from the crossed term. The peak of the distribution is still at around 1420 MeV, because the initial  $K^-p$  couples dominantly to the second pole of the  $\Lambda(1405)$ , although the width of this distribution is slightly larger than that of the I=0 resonance due to a finite contribution from the  $\Sigma(1385)$ .

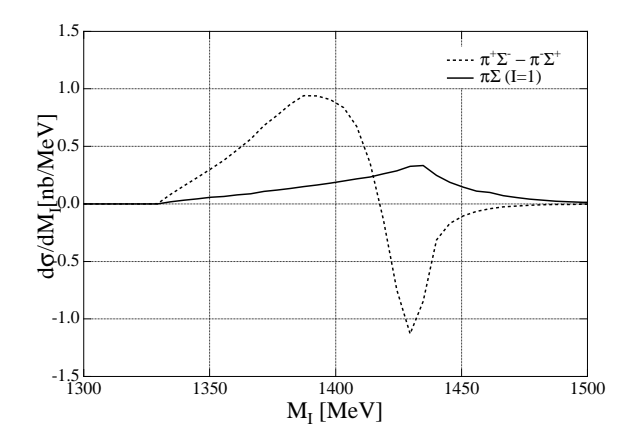


FIG. 5: Invariant mass distributions of  $\pi^+\Sigma^- - \pi^-\Sigma^+$  (Dashed), and s-wave,  $\pi\Sigma(I=1)$  (Solid), in units of [nb/MeV].

In the chiral unitary model, I=1 s-wave amplitude has an interesting feature: another pole is found at 1410-40i [9, 19]. However, the existence of this pole is sensitive to the details of the model, and in some cases, it appears in unphysical Riemann sheet. But in all cases, the reflection of the pole could be seen on the scattering line. Usually, the I=1 amplitude can be extracted by combining the three  $\pi\Sigma$  channels:

$$\frac{d\sigma(\pi^+\Sigma^-)}{dM_I} + \frac{d\sigma(\pi^-\Sigma^+)}{dM_I} - 2\frac{d\sigma(\pi^0\Sigma^0)}{dM_I} \propto |T^{(1)}|^2 . \quad (8)$$

However, the  $|T^{(1)}|^2$  term would contain contributions both from s and p-wave, although the contribution of the p-wave to the  $\pi\Sigma$  channels is small. In order to extract the I=1 s-wave amplitude, we can utilize the crossed term in Eq. (7). Since we are looking at the cross sections where the angle variable among MB is integrated, the product of s- and p-wave amplitude vanishes. Then, the difference of the distributions for the two charged states contains only the s-wave  $T^{(1)}$  amplitude

$$\frac{d\sigma(\pi^{+}\Sigma^{-})}{dM_{I}} - \frac{d\sigma(\pi^{-}\Sigma^{+})}{dM_{I}} = \frac{4}{\sqrt{6}} \operatorname{Re}(T_{s}^{(0)}(T_{s}^{(1)})^{*}) . \quad (9)$$

We plot this magnitude in Fig. 5 with a dashed line. In principle, it is possible to extract  $T_s^{(1)}$  from this quantity combining the distribution of s-wave I=0 (for instance, from the  $\pi^0\Sigma^0$ ). Theoretically, in the present framework, we can calculate the pure s-wave I=1 component by switching off the  $\Sigma(1385)$  and making the combination of  $\pi\Sigma$  amplitudes as in Eq. (8). The results are shown in Fig. 5 (Solid line) and a small peak is seen as a reflection of the approximate resonant structure predicted in Refs. [9, 19].

In summary, we have proposed a reaction  $\gamma p \to \pi^+ K^0 MB$  for the study of the second pole possibly existing in the  $\Lambda(1405)$  region. As expected, the mass distribution peaks at around 1420 MeV with a relatively narrow width, and the present reaction is suitable for the

isolation of the second pole. We have also shown that the effect of  $\Sigma(1385)$  resonance for the  $\pi\Sigma$  states is small enough to see the structure of second pole of  $\Lambda(1405)$ . The observation of different shapes of mass distribution from the nominal one, such as in  $\pi^-p \to K^0\pi\Sigma$  [25], can be the proof of the reflection of double pole structure. Experimental evidence on the existence of such two  $\Lambda^*$  states would provide more information on the nature of the current  $\Lambda(1405)$  and thus new clues to understand non-perturbative dynamics of QCD. For more details, see Ref. [23].

Japan-Europe (Spain) Research Cooperation Program of Japan Society for the Promotion of Science (JSPS) and Spanish Council for Scientific Research (CSIC), which enabled T. H. and A. H. to visit IFIC, Valencia and M.J.V. V. visit RCNP, Osaka. This work is also supported in part by DGICYT projects BFM2000-1326, and the EU network EURIDICE contract HPRN-CT-2002-00311.

comments and discussions. This work is supported by the

## Acknowledgments

We would like to thank Prof. T. Nakano for suggesting this work to us. We also thank Dr. D. Jido for useful

- R. H. Dalitz, T. C. Wong, and G. Rajasekaran, Phys. Rev. 153, 1617 (1967).
- [2] M. Jones, R. H. Dalitz, and R. R. Horgan, Nucl. Phys. B129, 45 (1977).
- [3] R. H. Dalitz and S. F. Tuan, Ann. Phys. (N.Y.) 10, 307 (1960).
- [4] N. Kaiser, P. B. Siegel, and W. Weise, Nucl. Phys. A594, 325 (1995).
- [5] N. Kaiser, T. Waas, and W. Weise, Nucl. Phys. A612, 297 (1997).
- [6] E. Oset and A. Ramos, Nucl. Phys. A635, 99 (1998).
- [7] M. F. M. Lutz and E. E. Kolomeitsev, Nucl. Phys. **A700**, 193 (2002).
- [8] Y. Nemoto, N. Nakajima, H. Matsufuru, and H. Suganuma, Phys. Rev. D68, 094505 (2003).
- [9] J. A. Oller and U. G. Meissner, Phys. Lett. **B500**, 263 (2001).
- [10] E. Oset, A. Ramos, and C. Bennhold, Phys. Lett. B527, 99 (2002).
- [11] D. Jido, A. Hosaka, J. C. Nacher, E. Oset, and A. Ramos, Phys. Rev. C66, 025203 (2002).
- [12] C. Garcia-Recio, J. Nieves, E. Ruiz Arriola, and M. J. Vicente Vacas, Phys. Rev. D67, 076009 (2003).
- [13] T. Hyodo, S. I. Nam, D. Jido, and A. Hosaka, Phys. Rev.

C68, 018201 (2003).

- [14] T. Hyodo, S. I. Nam, D. Jido, and A. Hosaka, nucl-th/0305011.
- [15] C. Garcia-Recio, M. F. M. Lutz, and J. Nieves, Phys. Lett. B582, 49 (2004)
- [16] S. I. Nam, H. -Ch. Kim, T. Hyodo, D. Jido, and A. Hosaka, hep-ph/0309017.
- [17] P. J. Fink Jr., G. He, R. H. Landau, and J. W. Schnick, Phys. Rev. C41, 2720 (1990).
- [18] A. Zhang et al., hep-ph/0403210.
- [19] D. Jido, J. A. Oller, E. Oset, A. Ramos, and U. G. Meissner, Nucl. Phys. A725, 181 (2003).
- [20] J. C. Nacher, E. Oset, H. Toki, and A. Ramos, Phys. Lett. **B455**, 55 (1999).
- [21] J. C. Nacher, E. Oset, H. Toki, and A. Ramos, Phys. Lett. **B461**, 299 (1999).
- [22] T. Hyodo, A. Hosaka, E. Oset, A. Ramos, and M. J. Vicente Vacas, Phys. Rev. C68, 065203 (2003).
- [23] T. Hyodo, A. Hosaka, M. J. Vicente Vacas, and E. Oset, nucl-th/0401051.
- [24] LEPS, J. K. Ahn, Nucl. Phys. A721, 715 (2003).
- [25] D. W. Thomas, A. Engler, H. E. Fisk, and R. W. Kraemer, Nucl. Phys. B56, 15 (1973).